



Synthesis, characterization, photophysical, and photochemical properties of novel phthalocyanines containing thymoxy groups as bioactive units

Rovshen Atajanov^{1,4} · Khaoula Khezami^{2,3} · Mahmut Durmuş² · Zafer Odabaş¹

Received: 27 November 2022 / Accepted: 2 March 2023 / Published online: 17 March 2023
© The Author(s), under exclusive licence to Springer Nature Switzerland AG 2023

Abstract

In this study, new 4-chloro-5-(2-isopropyl-5-methylphenoxy)phthalonitrile compound, containing bioactive thymoxy group, and its metal-free phthalocyanine and metallo-phthalocyanine derivatives were synthesized for the first time. Their structures were determined by spectroscopic methods such as FTIR, UV–Vis, ¹H-, and ¹³C-NMR (for phthalonitrile derivative), MALDI-TOF mass spectrometry (for phthalocyanine derivatives) and elemental analysis as well. The phthalocyanines showed excellent solubility in polar and nonpolar solvents without aggregation and absorb at long wavelengths with their high molar coefficient. In N,N-dimethylformamide, the effects of the type of central metal ions [metal-free, indium(III) acetate, lutetium(III) acetate, magnesium(II) or zinc(II)] in the phthalocyanine, containing bioactive thymoxy group, cavity on the spectroscopic, photophysical, and photochemical properties of the phthalocyanines were determined. These features are compared with each other. Lutetium(III) acetate phthalocyanine did not show any fluorescence, while metal-free phthalocyanine and indium(III) acetate phthalocyanine showed low fluorescence. It was determined that magnesium phthalocyanine significantly enriched the fluorescence, and zinc phthalocyanine had appropriate and sufficient fluorescence. Lutetium(III) acetate and zinc(II), especially indium(III) acetate phthalocyanines, could produce large amounts of singlet oxygen. Metal-free and magnesium phthalocyanines had the capacity to produce sufficient singlet oxygen (it means production of enough amount of singlet oxygen by a photosensitizer candidate during PDT applications). All phthalocyanines have sufficient and suitable photostability (it means an ideal photosensitizer should be stable under light irradiation until complete its PDT activation, and it should be decomposed after its PDT activation so that it does not accumulate in the body). With these determined properties, magnesium(II), especially indium(III) acetate and zinc(II) phthalocyanines, may be suitable candidates as type II photosensitizers for photodynamic therapy applications. Lutetium(III) acetate phthalocyanine may be a photosensitizer candidate in photocatalytic applications.

Introduction

Photodynamic therapy (PDT) is a well-known method based on the interaction of light, photoactive material, and oxygen, and commonly used to treat of many cancer (tumor) diseases and to control bacterial invasion in bacterial diseases [1–4]. In this method, the phototherapeutic agent, also called photosensitizer (PS), is firstly deposited in the tumor tissue, irradiated with light, and then, the oxygen in the cell reacts with this enriched agent (PS) and leads to the excitation of PS. Thus, the excited photosensitizer transfers spin-permissible energy to the cell, and the singlet oxygen occurs there. Last, highly reactive singlet oxygen can occur in reaction with the damaged tissue and cause the death of the tumor [5].

Despite the successes of first-generation PS such as Photofrin®, Photosan®, and some hematoporphyrin derivatives,

✉ Zafer Odabaş
zodabas@marmara.edu.tr

¹ Department of Chemistry, Marmara University,
34722 Kadıköy, Istanbul, Turkey

² Department of Chemistry, Gebze Technical University,
41400 Gebze, Kocaeli, Turkey

³ Topkapı Campus, İstinye University,
31010 Zeytinburnu, Istanbul, Turkey

⁴ Mads Clausen Institute, SDU CAPE, University of Southern
Denmark, 6400 Sønderborg, Denmark

scientists have been searched to new compounds that meet the demands of modern medicine. Important aspects for ideal photosensitizers are absorption in the long-wave range, high absorption coefficients, and stability during irradiation. In addition, second-generation PSs should have the features of rapid tumor accumulation, low dark toxicity, and a broad spectrum of activity [5–8]. A class of compounds that fulfills these properties in many ways is phthalocyanines (Pcs). Since the early 1980s, these macrocycles have been considered potential sensitizers for PDT and are the subject of intense research [9].

Pcs have been a major source of interest since the discovery of their unexpected synthesis at the beginning of the last century [10]. The reason for the intense interest in these macrocycles is because of their high stability, architectural flexibility, and unique spectral properties [11]. Due to the ease of the modifications on the Pc ring, optional adjustments can be made to improve their properties. For example, Pc aggregation can be decreased, and Pc solubility can be enhanced by introducing bulky groups with alkyl chains to the axial and peripheral positions of the Pcs. On the other hand, while the hydrogen atoms in the Pc core can be replaceable by more than 70 different metals and metalloids. This advantage offers additional features for synthetic organic chemists to optimize the physical responses of the Pcs [12].

Pcs have special photochemical properties due to the location of the highest occupied molecular orbital (HOMO) and lowest unoccupied molecular orbital (LUMO) energy levels and their energy difference (ΔE). Since the molecular orbitals are quantized in terms of their energy, Pcs absorb the photons of certain energy ($h\nu$). The energy of photons is equal to the difference in energy ($\Delta E = h\nu$) between the ground and excited states. Since the HOMO/LUMO energy difference of the Pcs is ~ 170 kJ/mol (~ 700 nm), Pcs can be excited by visible light [9, 13–18].

The photochemical generation of singlet oxygen takes place after the triplet singlet energy transfer due to the photosensitizers such as Pcs, porphyrins, rose Bengal, methylene blue, or chlorophyll [19].

The triplet energy for the porphyrins and Pcs is approx. 108–150 kJ/mol. The energies of the first excited state ($1\Delta_g$) and the second excited state ($1\Sigma_g^+$) of oxygen are 94.7 kJ/mol and 157.8 kJ/mol, respectively. The energy of the excited state of oxygen is therefore below the energy of the triplet state of these photosensitizer. This is one of the most important conditions for energy transfer [20].

Thymol and its derivatives have been studied extensively because of their biological activities. Thymol is a phenolic monoterpenoid compound obtained from essential oils of *Thymus vulgaris*, *Monarda punctata* [21], and various other kinds of plants. It shows wide biological activities against cancerogenic cells [22] and microbial diseases [23]. It has been known

to exhibit anti-inflammatory [24] and anti-oxidative effects [25]. In fact, studies on alpha and beta substituted thymoxy substituted Pcs are also found in the literature [26, 27]. However, these species (alpha and beta tetra-substituted Pcs) form regioisomers during their synthesis process. It is extremely difficult to separate four obtained isomers from each other, and only HPLC method can most effectively be separate this isomer mixture [28]. Pc researchers who prefer these syntheses often and isolate the most abundant species in the mixture and can study its properties [27]. The properties of other isomers are often not determined due to lack of quantity [27]. However, octa thymoxy substituted Pcs obtained as a single isomer by using disubstituted starting phthalonitriles are not available in the literature. It was determined in the literature about the synthesis of octa thymoxy substituted Pcs that the starting material (4,5-bis(2-isopropyl-5-methylphenoxy)phthalonitrile) was synthesized, but no Pc synthesis was made using this substance [16]. Thus, syntheses of octa substituted Pcs, contain at peripheral positions a thymoxy and a chlorine groups, were planned by using 4-chloro-5-(2-isopropyl-5-methylphenoxy) phthalonitrile starting compound in this study (Scheme 1). It is predicted that the addition of the electron-withdrawing chlorine groups to the molecular structure will show different chemical, physical, and photophysical properties compared to alpha or beta tetra thymoxy substituted Pc in the literature. It is predicted that since electron-withdrawing chlorine groups added to the molecular structure, these Pcs will show different chemical, physical and photophysical properties compared to alpha or beta tetra thymoxy substituted Pcs in the literature.

Experimental

Materials and method

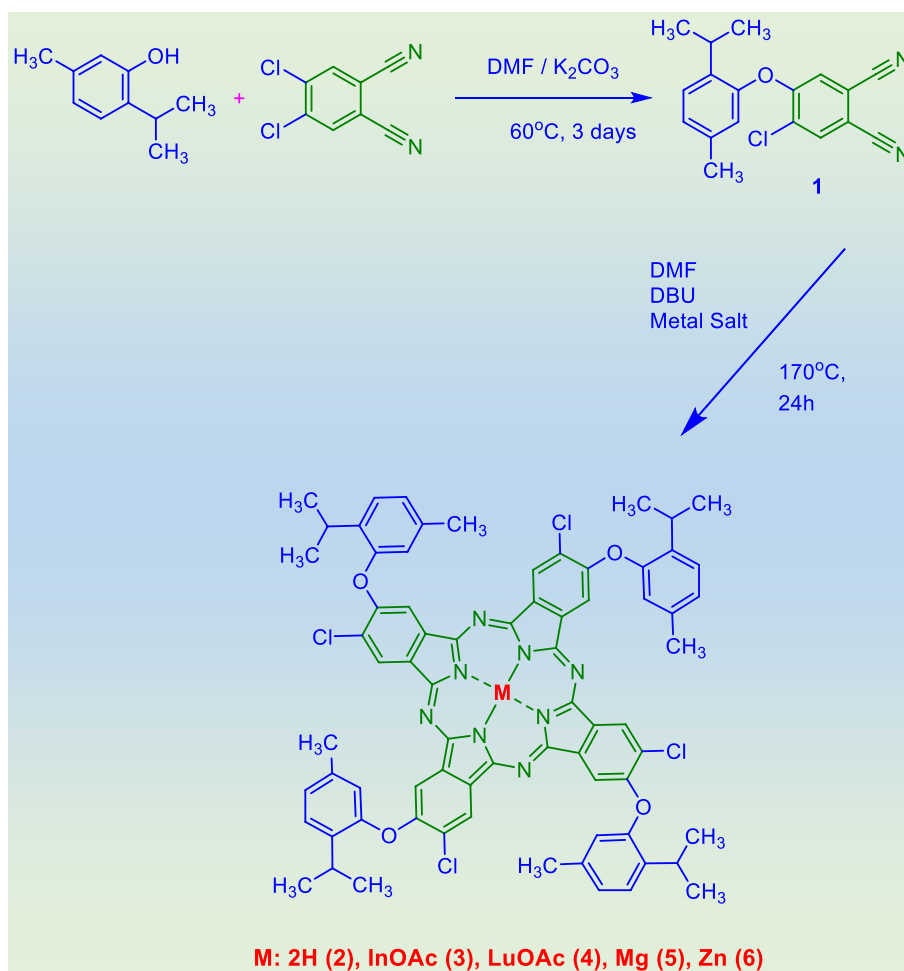
In this study, thymoxy substituted phthalonitrile compound (1) was synthesized by a nucleophilic aromatic substitution reaction between thymol and 4,5-dichlorophthalonitrile [29] and its metal-free and metallo-Pcs (2–6) were obtained by using this compound. The materials and equipment are given in the supplementary information section.

Synthesis

4-Chloro-5-(2-isopropyl-5-methylphenoxy) phthalonitrile (1)

Solution of thymol (2-isopropyl-5-methylphenol) (1.5 g, 10 mmol) in 20 mL dry DMF was slowly added while stirring to the solution of 4,5-dichlorophthalonitrile (1.97 g, 10 mmol) in 30 mL dry DMF and the solution stirred further for 15 min. Afterward, finely powdered K_2CO_3 (2.76 g, 20 mmol) was added to this medium. The reaction solution

Scheme 1 Synthetical pathway of phthalonitrile compound (**1**) and its metal-free (**2**) and metallo (**3–6**) phthalocyanines



was stirred at 60 °C for 3 days under a vacuum. The reaction was followed by thin-layer chromatography (TLC) and stopped after the disappearance of spots belonging to the reactants on the TLC plate. The reaction mixture was cooled, and K_2CO_3 was filtered. The filtrate was then poured into ice water. After the complete precipitation, the crude product was filtered with a sand funnel and washed several times with water. Compound **1** was purified by column chromatography (silica gel) using $CHCl_3$ as an eluent. The collected fraction was dried to obtain pure compound **1** in a good yield (71%) [29].

Compound **1** is soluble in dichloromethane (DCM), $CHCl_3$, tetrahydrofuran (THF), acetonitrile, acetone, toluene, DMF, and dimethyl sulfoxide (DMSO). Yield: 2.2 g (71%). Melting point: 124–126 °C. FTIR ν_{max} (cm^{-1}): 523, 610, 826, 959, 1020, 1069, 1094, 1179, 1246, 1364, 1420, 1486, 1514, 1588, 1607, 2233, 2848, 2965, 3046, 3080. 1H -NMR (500 MHz, $DMSO-d_6$) δ , ppm: 8.54 (s, 1H), 7.44 (s, 1H), 7.34 (d, $J=7.8$ Hz, 1H), 7.12 (d, $J=7.8$ Hz, 1H), 6.88 (s, 1H), 2.96 (septet, $J=6.9$ Hz, 1H), 2.28 (s, 3H), 1.14 (d, $J=6.9$ Hz, 6H). ^{13}C -NMR (500 MHz, $CDCl_3$) δ , ppm: 158.5 (1C), 151.0 (1C), 139.0 (1C), 136.9 (1C), 135.5

(1C), 128.9 (1C), 128.0 (1C), 128.0 (1C), 120.9 (1C), 119.6 (1C), 116.0 (1C), 114.7 (1C), 114.6 (1C), 110.9 (1C), 27.3 (1C), 22.9 (1C), 22.8 (2C). Elemental analysis: % calculated for $C_{18}H_{15}ClN_2O$: C, 69.57; H, 4.87; N, 9.01, obtained % results: C, 69.74; H, 4.69; N, 9.16[29].

2,9,16,23-tetrachloro-3,10,17,24-tetrakis(2-isopropyl-5-methylphenoxy)phthalocyanine (H_2Pc) (**2**)

4-Chloro-5-(2-isopropyl-5-methylphenoxy)phthalonitrile (**1**) (0.93 g, 3 mmol) and lithium (0.03 g, 4 mmol) in n-pentanol (20 mL) were mixed and stirred at 150 °C for 18 h under N_2 atmosphere. This solution was cooled to room temperature. Then, the solvent was evaporated under a vacuum. Then, CH_3COOH (30 mL) was added, and the suspension was stirred for 30 min. The product was extracted with dichloromethane and washed with water (3×30 mL). The organic phase is separated and dried with anhydrous magnesium sulfate.

Compound **2** is soluble in hexane, DCM, $CHCl_3$, THF, acetonitrile, acetone, toluene, DMF, and DMSO. Yield: 0.24 g (26%). Melting point ≈ 300 °C. FTIR ν_{max} (cm^{-1}): 436,

460, 586, 688, 737, 811, 881, 937, 1011, 1084, 1147, 1246, 1417, 1502, 1575, 1603, 2014, 2161, 2554, 2867, 2924, 2959, 3028, 3286. UV–Vis (DCM, 1×10^{-5} M): λ_{\max} (nm) (log ϵ): 701 (5.05), 667 (5.03), 637 (4.71), 608 (4.56), 347 (4.91). Elemental analysis: % calculated for $C_{72}H_{62}Cl_4N_8O_4$: C, 69.52; H, 5.06%; N, 14.45, obtained % results: C, 69.41; H, 5.13; N, 14.30. MS: (MALDI-TOF), m/z calc. 1245.14, found 1245.74 $[M]^+$.

General synthesis procedure for the metallo-phthalocyanines

4-Chloro-5-(2-isopropyl-5-methylphenoxy)phthalonitrile (**1**) (0.93 g, 3 mmol) and metal salt (0.58 g indium(III) acetate for **In(OAc)Pc**, 0.73 g lutetium(III) acetate hydrate for **Lu(OAc)Pc**, 0.43 g magnesium acetate tetrahydrate for **MgPc**, 0.37 g zinc acetate dihydrate for **ZnPc**), and 0.2 mL of DMF were evacuated into a Schlenk tube and stirred until all solids had dissolved. Then, 1,8-diazabicyclo[5.4.0]undec-7-ene (DBU) (0.35 mL, 2.34 mmol) was added dropwise to the reaction tube while stirring. The reaction mixture was stirred at 160 °C under an inert atmosphere overnight. After cooling to room temperature, the reaction solution was poured onto 450 mL of methanol/water (8: 1) and the formed solids were filtered. The crude product was washed with water overnight and methanol in a Soxhlet apparatus. The resulting solid was purified by column chromatography (silica gel) with $CHCl_3/MeOH$ (20:1) solvent system as an eluent. Green pure products were obtained.

2,9,16,23-Tetrachloro-3,10,17,24-tetrakis(2-isopropyl-5-methylphenoxy)phthalocyaninato indium(III)acetate (In(OAc)Pc) (3) Compound **3** is soluble in DCM, $CHCl_3$, THF, ethanol, acetone, toluene, DMF, and DMSO. Yield: 0.18 g (19%). Melting point >300 °C. FTIR ν_{\max} (cm^{-1}): 439, 555, 586, 744, 814, 944, 993, 1060, 1084, 1147, 1246, 1330, 1389, 1435, 1505, 1572, 1603, 1649, 1718, 2851, 2867, 2924, 2959, 3052. UV–Vis (DMSO, 1×10^{-5} M): λ_{\max} (nm) (log ϵ): 693 (4.96), 626 (4.30), 366 (4.72). Elemental analysis: % calculated for $C_{74}H_{63}Cl_4N_8O_4In$: C, 62.73; H, 4.48; N, 7.91, obtained % results: C, 62.61; H, 4.33; N, 8.03. MS: (MALDI-TOF), m/z calc. 1416.99, found 1359.38 $[M-OAc+H]^+$.

2,9,16,23-Tetrachloro-3,10,17,24-tetrakis(2-isopropyl-5-methylphenoxy)phthalocyaninato lutetium(III)acetate (Lu(OAc)Pc) (4) Compound **4** is soluble in hexane, DCM, $CHCl_3$, THF, ethanol, acetone, toluene, DMF, and DMSO. Yield: 0.20 g (21%). Mp: >300 °C. FTIR ν_{\max} (cm^{-1}): 432, 474, 586, 678, 751, 811, 888, 944, 993, 1056, 1084, 1147, 1246, 1389, 1435, 1568, 1719, 1607, 1656, 1719, 2867, 2924, 2960, 3018. UV–Vis (DMSO, 1×10^{-5} M): λ_{\max} (nm) (log ϵ): 685 (5.06), 614 (4.33), 358 (4.77). Elemental

analysis: % calculated for $C_{74}H_{63}Cl_4N_8O_4Lu$: C, 60.17; H, 4.30; N, 7.59, obtained % results: C, 60.31; H, 4.43; N, 7.73. MS: (MALDI-TOF), m/z calc. 1477.13, found 1418.07 $[M-OAc+H]^+$.

2,9,16,23-Tetrachloro-3,10,17,24-tetrakis(2-isopropyl-5-methylphenoxy) phthalocyaninato magnesium (5) Compound **5** is soluble in hexane, DCM, $CHCl_3$, THF, ethanol, acetone, toluene, DMF, and DMSO. Yield: 0.30 g (32%). M.p. >300 °C. FTIR ν_{\max} (cm^{-1}): 432, 492, 590, 695, 748, 807, 884, 941, 986, 1053, 1088, 1151, 1242, 1333, 1389, 1424, 1498, 1572, 1603, 1663, 2856, 2919, 2954, 3024. UV–Vis (DMSO, 1×10^{-5} M): λ_{\max} (nm) (log ϵ): 680 (4.96), 615 (4.42), 358 (4.71). Elemental analysis: % calculated for $C_{72}H_{60}Cl_4N_8O_4Mg$: C, 68.23; H, 4.77; N, 8.84, obtained % results: C, 68.31; H, 4.54; N, 8.73. MS: (MALDI-TOF), m/z calc. 1267.43, found 1266.57 $[M-H]^+$.

2,9,16,23-Tetrachloro-3,10,17,24-tetrakis(2-isopropyl-5-methylphenoxy) phthalocyaninato zinc (6) Compound **6** is soluble in hexane, DCM, $CHCl_3$, THF, ethanol, acetone, toluene, DMF, and DMSO. Yield: 0.33 g (35%). FTIR ν_{\max} (cm^{-1}): 446, 692, 741, 804, 881, 941, 990, 1056, 1084, 1147, 1246, 1333, 1382, 1428, 1481, 1568, 1603, 1656, 2863, 2919, 2961, 3038. UV–Vis (DMSO, 1×10^{-5} M): λ_{\max} (nm) (log ϵ): 681 (5.01), 628 (4.53), 354 (4.78). Elemental analysis: % calculated for $C_{72}H_{60}Cl_4N_8O_4Zn$: C, 66.09; H, 4.62; N, 8.56, obtained % results: C, 66.27; H, 4.55; N, 8.72. MS: (MALDI-TOF), m/z calc. 1308.50, found 1308.81 $[M]^+$.

Results and discussion

Synthesis and characterization

4-Chloro-5-(2-isopropyl-5-methylphenoxy)phthalonitrile (**1**) compound was obtained by the nucleophilic substitution reaction between thymol and 4,5-dichlorophthalonitrile[29]. In the 1H -NMR spectrum of this compound, aliphatic hydrogen peaks of isopropyl and methyl groups on the molecule can be seen clearly. Moreover, ortho and meta splitting of Ar–H peaks can be easily distinguished between 7 and 7.5 ppm (Fig. S1 in the SI). In the ^{13}C -NMR spectrum of this compound, aliphatic carbons (4C) peaks, aromatic carbons (12C) peaks, and nitrile carbons (2C) peaks were observed at 22.8–27.3 ppm, 110.9–158.5 ppm, and 114.6 ppm, respectively (Fig. S2 in the SI). The functional groups of the phthalonitrile molecule were verified by FTIR spectroscopy, and it was observed peaks between 2869 and 2972 cm^{-1} for aliphatic C–H, 3036–3100 cm^{-1} for aromatic C–H, the sharp peak at 2234 cm^{-1} for nitrile (C≡N) vibration, and moreover,

the aromatic O–H peak of thymol was disappeared in the FTIR spectrum of compound **1** (Fig. S3 in the SI) [29].

Metallo- and metal-free Pcs were synthesized from the anhydrous basic tetramerization reaction of the phthalonitrile compound **1**. The structures of Pcs were checked by employing common spectroscopic techniques such as FTIR, UV–Vis, MALDI-TOF mass spectrometry and elemental analyses as well.

The nitrile stretching peak was disappeared in the FTIR spectra of the Pcs after the tetramerization reaction. The aromatic and aliphatic C–H stretching peaks were observed between 3052–3018 cm^{-1} and 2932–2907 cm^{-1} in the FTIR spectra, respectively. The characteristic N–H stretching peak of metal-free phthalocyanine (**H₂Pc**) was observed at 3286 cm^{-1} as an extra peak (Figs. S4, S6, S8, S10, and S12 in the SI). In addition, C=O stretching bands were observed at 1718 and 1719 cm^{-1} , respectively, in the FTIR spectra of In(OAc)Pc and Lu(OAc)Pc. This situation can be attributed to the fact that these metals with +3 oxidation states attach acetate groups from their axial bonds in Pc molecules.

The MALDI-TOF mass spectra of the Pcs were accurate with the proposed structures. The molecular ion peaks for **H₂Pc** (**2**), **MgPc** (**5**), **ZnPc** (**6**) and [M–OAc + H]⁺ fragmented ion peaks for **In(OAc)Pc** (**3**) and **Lu(OAc)Pc** (**4**) were easily identified at *m/z*: 1245.74 as [M⁺], 1266.57 as [M–H]⁺, 1308.81 as [M⁺], 1359.38 as [M–OAc + H]⁺, and 1418.07 as [M–OAc + H]⁺, respectively (Figs. S5, S7, S9, S11 and S13 in the SI). All results mentioned above confirmed that the synthesis of the compounds was accomplished. All the above-mentioned results confirmed that the synthesis of the compounds was successfully achieved.

Photophysical and photochemical properties

Electronic absorption and fluorescence spectra

To be able to penetrate deeper into the tissue with light, the photosensitizers must have long-wavelength absorption maxima and high molar extinction coefficients. A 600–800 nm absorption window is optimal for a photosensitizer for PDT treatment. Molecules with absorption maxima above 850 nm have triplet states that have too low energy and cannot be used for medical purposes, since the energy of light ($\lambda = 850 \text{ nm}$) is not sufficient to generate singlet oxygen.

Thymol-substituted Pcs (**2–6**) showed two major characteristic absorption bands called as B and Q between 347–358 nm and 681–701 nm, respectively, caused by the $\pi-\pi^*$ transition. As a result of D_{2h} symmetry, **H₂Pc** exhibited typical metal-free Pc spectral behavior with two narrow peaks in the Q region band at 667 and 701 nm. While it shows monomeric behavior in chloroform, dichloromethane,

DMF, THF, and toluene, it forms aggregates in acetone, and hexane (Fig. S14 in the SI).

The photophysical properties affect negatively when a photosensitizer forms aggregates. In addition, aggregated molecules have greatly altered solubility properties, which can cause difficulties at the cellular level. In particular, the formation of H-aggregates should be avoided. For this reason, the photosensitizer must be structurally modified so that aggregates in the solution are as unstable as possible. This problem can be overcome through the introduction of bulky substituents on the phthalocyanine ring. The formation of J aggregation instead of H-aggregates in a solution can be decisive for a photosensitizer for the potential application in PDT. However, the tendency to form aggregates in solution is difficult to predict and must always be examined very carefully.

In the aggregation studies of the synthesized metallo-Pcs (**3–6**), all the compounds showed quite similar behavior and tend not to aggregate in common organic solvents, except for **MgPc**, which showed J-aggregation in chloroform solutions, **In(OAc)Pc** and **ZnPc** which indicates H-aggregated species in ethanol solutions (Figs. S15, S16, S17 and S18 in the SI). DMF was chosen as a solvent for further photophysical and photochemical properties. The fact that the Q bands are very narrow suggests very little aggregation of the molecules in the concentration range investigated, which confirms the thymol-substituted Pcs (**2–6**) avoid $\pi-\pi$ stacking interactions. The aggregation properties of the synthesized compounds were investigated at different concentrations ranging from 1×10^{-5} to 1×10^{-6} M in DMF (Figs. 1, 2, and S19, S20, and S21 in the SI). Any of the Pcs do not aggregate in DMF solutions. The small amount of DMF is not toxic in the biological environment, and its miscibility with water is another advantage of this solvent for PDT studies.

Fluorescence emission peaks maxima of the studied Pcs (**2–6**) are listed in Table 1. Figures 3, 4, S22, and S23 in the SI show the absorption, fluorescence emission, and excitation spectra of peripherally thymol and chlorine-bearing Pcs (**2–6**) in DMF. The Stokes shifts of the studied Pcs (**2–6**) were observed to be slightly longer in comparison with unsubstituted **ZnPc**, and they were found in the range of 7–10 nm. The similarity between excitation and absorption spectra of the Pcs can be explained by the no effect of the used light during excitation.

Fluorescence quantum yields

An ideal photosensitizer should show some fluorescence behavior to be able to follow them in the body. Consequently, it is important to investigate fluorescence quantum yield (Φ_F) characteristics of photosensitization for PDT applications.

Fig. 1 UV–Vis electronic absorption spectra of 2,9,16,23-tetrachloro-3,10,17,24-tetrakis(2-isopropyl-5-methylphenoxy)phthalocyaninato magnesium (**5**) at different concentrations in DMF

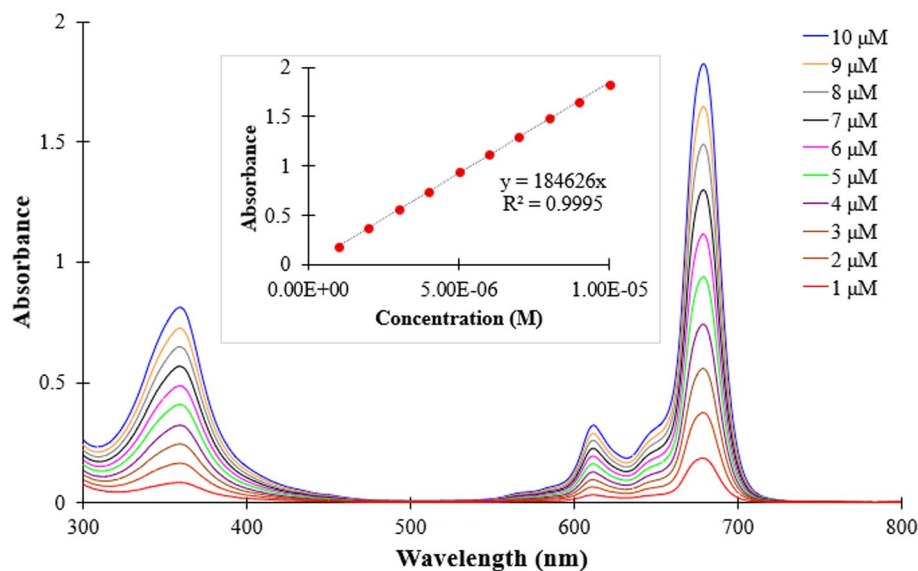


Fig. 2 UV–Vis electronic absorption spectra of 2,9,16,23-tetrachloro-3,10,17,24-tetrakis(2-isopropyl-5-methylphenoxy)phthalocyaninato zinc (**6**) at different concentrations in DMF

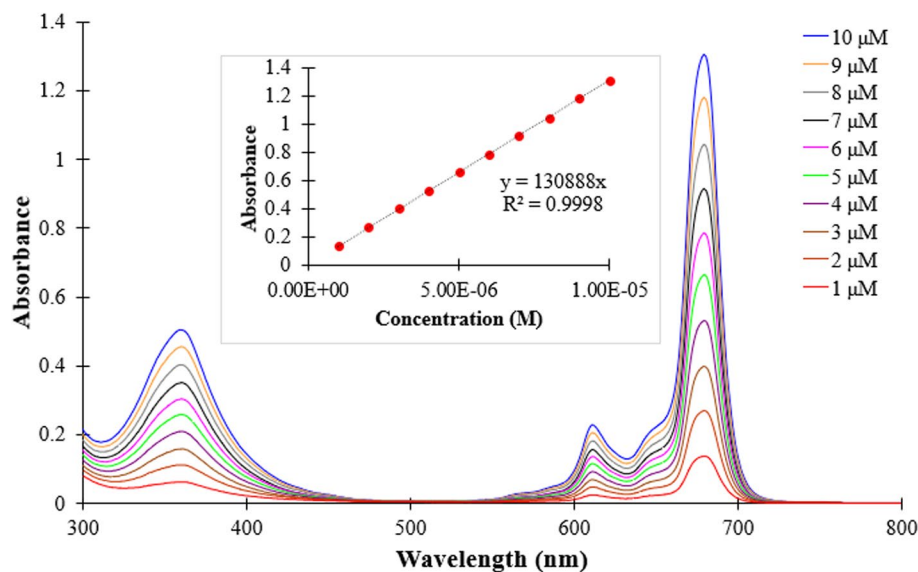


Table 1 Photophysical and photochemical data of the studied phthalocyanines (**2–6**) in DMF

| Compound | Q band λ_{\max} , (nm) | (log \mathcal{E}) | Excitation λ_{Ex} , (nm) | Emission λ_{Em} , (nm) | Stokes shift Δ_{Stokes} , (nm) | Φ_{F} | $\Phi_{\text{d}} (\times 10^{-4})$ | Φ_{Δ} |
|--------------------------------|--------------------------------------|----------------------|--|--|---|-------------------|------------------------------------|-----------------|
| H ₂ Pc (2) | 674 | 4.83 | 679 | 686 | 7 | 0.075 | 3.01 | 0.13 |
| In(OAc)Pc (3) | 691 | 4.91 | 689 | 699 | 10 | 0.051 | 4.32 | 0.84 |
| Lu(OAc)Pc (4) | 680 | 5.16 | – | – | – | – | 1.14 | 0.80 |
| ZnPc (6) | 679 | 5.11 | 678 | 687 | 9 | 0.138 | 1.10 | 0.70 |
| MgPc (5) | 679 | 5.26 | 678 | 685 | 7 | 0.345 | 3.32 | 0.26 |
| Std–ZnPc ^a | 670 | 5.37 | 670 | 676 | 6 | 0.17 | 0.23 | 0.56 |

^aReference from [30]

Fig. 3 Excitation, emission and absorption spectra of 2,9,16,23-tetrachloro-3,10,17,24-tetrakis(2-isopropyl-5-methylphenoxy)phthalocyaninato magnesium (**5**) (Solvent: DMF, $C = 1 \times 10^{-6}$ M). Excitation wavelength 646 nm

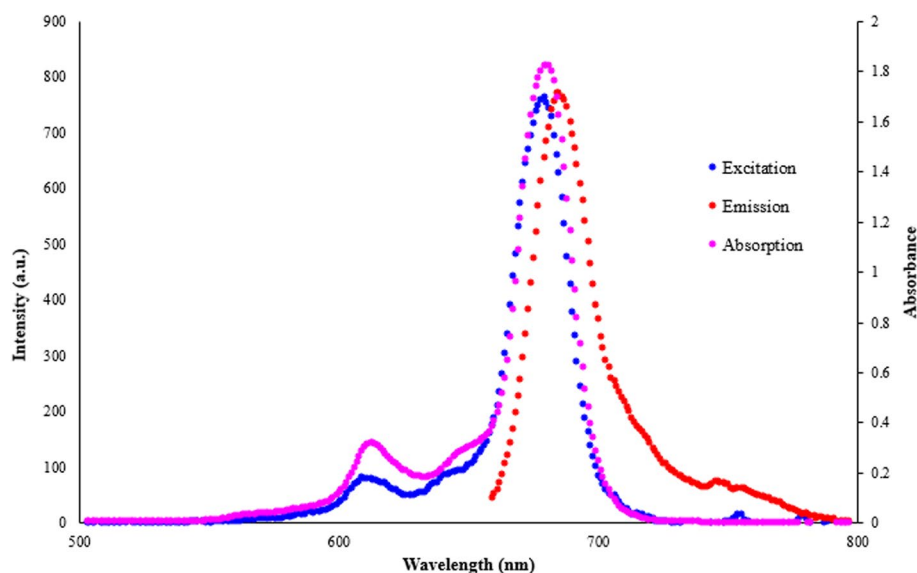
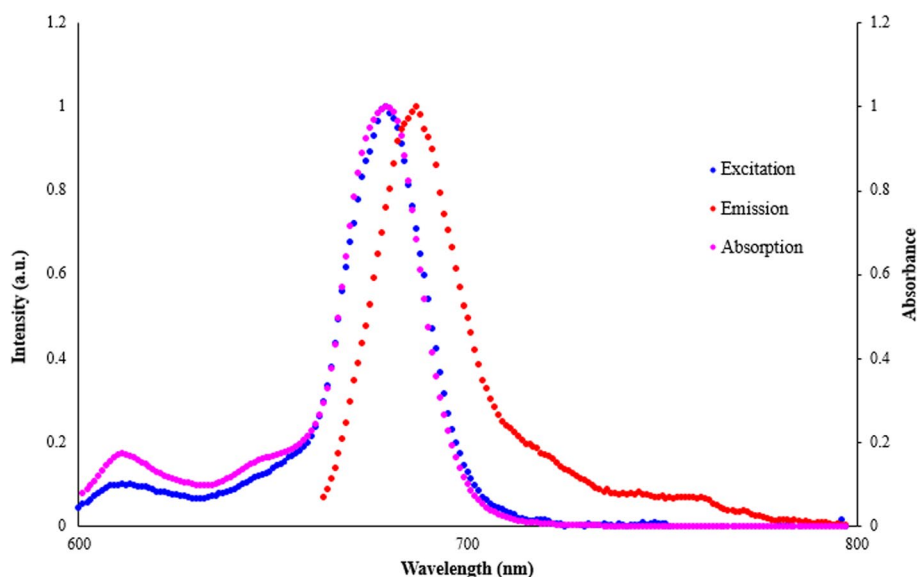


Fig. 4 Excitation, emission and absorption spectra of 2,9,16,23-tetrachloro-3,10,17,24-tetrakis(2-isopropyl-5-methylphenoxy)phthalocyaninato zinc (**6**) (Solvent: DMF, $C = 1 \times 10^{-6}$ M). Excitation wavelength 650 nm



The Φ_F values of the thymol-substituted Pcs (**2–6**) were determined in DMF, and the results are provided in Table 1. Φ_F value of Std-ZnPc was also supplied as a reference in this table for comparison in fluorescence quantum yield determinations. It can be concluded from the similarities of the absorption and excitation spectra of the studied compounds that the nuclear configurations of ground and excited states of the compounds are also similar and not affected by excitation (Figs. 3 and 4). The fluorescence quantum yields of the newly synthesized Pcs were obtained to be lower than the value of Std-ZnPc except for **MgPc**, which has the highest Φ_F value with a yield of 0.345. The high Φ_F value of **MgPc** can be explained by the bivalency, monoatomic dication, and

small ionic radius of the central metal, which diminishes the intersystem crossing to the triplet state. On the other hand, properties like high coordination number, big atomic radius, and trivalency of central metal of **In(OAc)Pc** make it less fluorescent compared to others. Due to the heavy atom effect of the lutetium(III) metal in the Pc cavity, no fluorescence emission was observed in the DMF solution of the compound **Lu(OAc)Pc**. Heavy metals increase intersystem crossing; therefore, less or no fluorescence is observed. Relatively low fluorescence quantum yield of **H₂Pc** ($\Phi_F = 0.075$) was observed compared to non-heavy metal Pcs (**5** and **6**) which might be the case of less fluorescence quenching for these metallo-Pcs **5** and **6**.

Singlet oxygen quantum yields (Φ_{Δ})

The singlet oxygen formed in the tissue generates oxidative cellular damage, which leads to apoptosis or necrosis of the affected tumor cells. Irradiation with a specific wavelength of light converts the photosensitizer into an excited state. This exciting photosensitizer collides with molecular triplet oxygen contained in the surrounding tissue. Ultimately, the photosensitizer returns to its ground state, and the cycle can repeat itself with continued exposure to light.

Since the intracellular generation of $^1\text{O}_2$ is the basis of PDT, it stands to reason that type II photoreaction is the focus of the further development of modern photosensitizers [30]. To obtain a high singlet oxygen quantum yield, the excited triplet state must be as long-lived as possible. This can be achieved by introducing heavy atoms, such as halogen atoms, or by introducing central atoms that stabilize the triplet state.

To calculate the singlet oxygen produced by the photosensitizer, 1,3-diphenylisobenzofuran (DPBF) is used as a singlet oxygen quencher. The quantum yield for the reaction between DPBF and singlet oxygen (Φ_{DPBF}) is determined experimentally from the decrease in DPBF absorbance at 417 nm after each irradiation interval.

The Φ_{Δ} values of the thymol-substituted Pcs (2–6) were determined in DMF, and the results are provided in Table 1. Φ_{Δ} value of Std-ZnPc was also supplied in Table 1 for comparison in singlet oxygen quantum yields of the studied Pcs (2–6). From the measurements of all the studied compounds, a significant decrease in the maximum absorption bands of DPBF was observed but there was not any change in the Q bands of Pcs, which shows the production of the singlet oxygen and stabilities of the photosensitizer compounds during

the photodynamic activity, respectively (Figs. 5, 6 and S24, S25 and S26 in the SI). Singlet oxygen quantum yields of **H₂Pc** and **MgPc** were found lower than that of Std-ZnPc, but these values were found to be higher for **ZnPc** and the highest for **In(OAc)Pc**. The lowest singlet oxygen generation efficiency with the Φ_{Δ} value of 0.13 was observed from the measurements of **H₂Pc** in DMF solution due to the lack of metal ions in the cavity. Mg and Zn Pcs can form two different forms of coordination depending on the reaction conditions. The first one is the square planar coordination in which the central Mg(II) and Zn(II) cations coordinate with the four isoindole nitrogen atoms of the Pc ring. The second one is the distorted tetragonal bi-pyramid coordination in which the central Mg(II) and Zn(II) cations coordinate by binding extra two acetate anions belonging to the salts at the axial positions of the Pc ring (4 + 2 coordination) [31]. In this study, when the FTIR spectra of the MgPc and ZnPc were examined, the band of the C=O bond was not observed belonging to the acetate group at around 1700 cm^{-1} . Thus, the result showed that the coordination of synthesized MgPc and ZnPc in this study is square planar. **MgPc** has a low Φ_{Δ} value because of the central metal magnesium, which is an alkaline earth metal divalent metal cation. Therefore, magnesium metal in the core of the Pc decreases the efficiency of the generation of singlet oxygen. On the other hand, **ZnPc** has a high Φ_{Δ} value of 0.70 compared to 0.56 of unsubstituted Std-ZnPc. It shows that both peripheral substituted thymol groups and the central metal zinc have an increasing effect on the singlet oxygen generation. The highest singlet oxygen generation efficiencies were observed for **In(OAc)Pc** and **Lu(OAc)Pc**, 0.84 and 0.80, respectively, which suggests the enhancing effect of heavy metals on the photochemical singlet oxygen production.

Fig. 5 Electronic absorption changes during the determination of singlet oxygen quantum yield of 2,9,16,23-tetrachloro-3,10,17,24-tetrakis(2-isopropyl-5-methylphenoxy)phthalocyanine (**2**) in DMF, $C = 1 \times 10^{-5}\text{ M}$

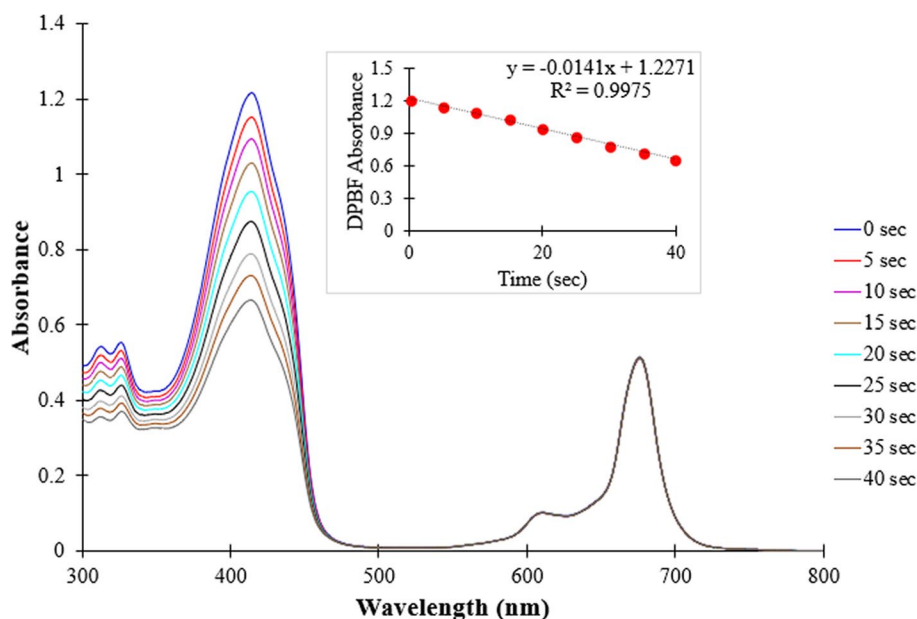
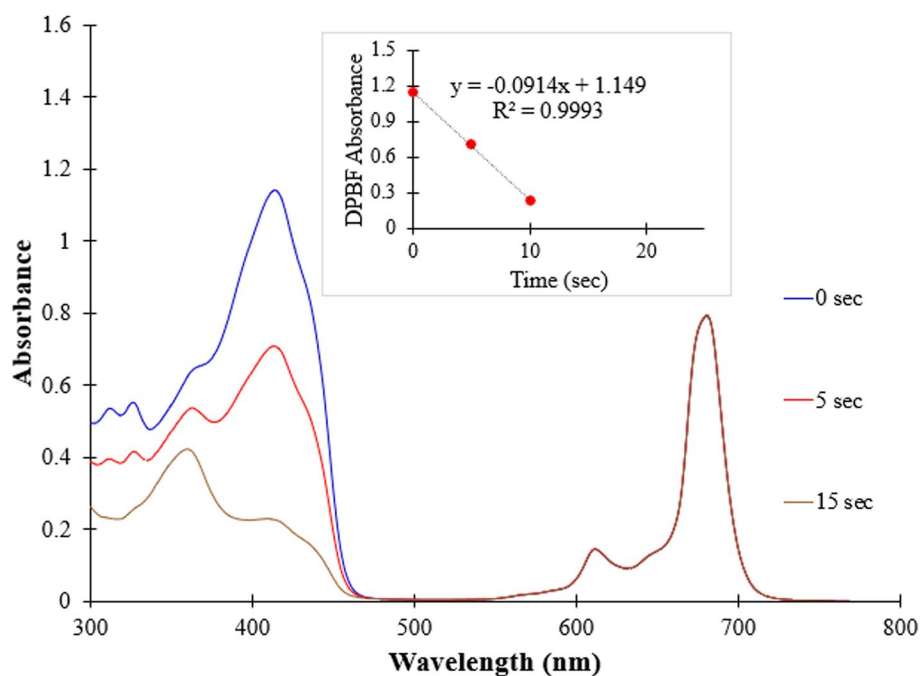


Fig. 6 Electronic absorption changes during the determination of singlet oxygen quantum yield of 2,9,16,23-tetrachloro-3,10,17,24-tetrakis(2-isopropyl-5-methylphenoxy)phthalocyaninato lutetium(III)acetate (**4**) in DMF, $C = 1 \times 10^{-5}$ M



Photodegradation studies

In the case of PDT, substances are required that have rather low photooxidative stability and also dark stability. In this way, a photosensitizer can be broken down in the body more quickly after irradiation. Photostabilities of the studied compounds were examined by evaluation of changes in their Q bands when they were exposed to a 50 V light at certain intervals (Figs. 7, 8 and S27, S28, and S29 in the SI). Photodegradation quantum yield (Φ_d) values obtained from those spectra help us to interpret PS's stability when exposed to light. Ideal photosensitizers

should be in a certain range of stability because it is necessary to avoid their toxicity within the body after the completion of the photodynamic action. Photodegradation quantum yields of stable **ZnPcs** are around 10^{-6} , and it is around 10^{-3} for unstable ones [17]. The observed Φ_d values of the studied thymol-substituted Pcs were higher than the unsubstituted Std-ZnPc ($\Phi_d = 0.23 \times 10^{-4}$) in DMF which implies a decrease in stability because of peripheral substitution. Photodegradation quantum yield (Φ_d) values of the thymol-substituted Pcs were found between 1.10×10^{-4} and 4.32×10^{-4} , which are acceptable values for their application in PDT.

Fig. 7 Electronic absorption spectral changes during the investigation of the photodegradation quantum yield of 2,9,16,23-tetrachloro-3,10,17,24-tetrakis(2-isopropyl-5-methylphenoxy)phthalocyaninato indium(III)acetate (**3**) in DMF, $C = 1 \times 10^{-5}$ M

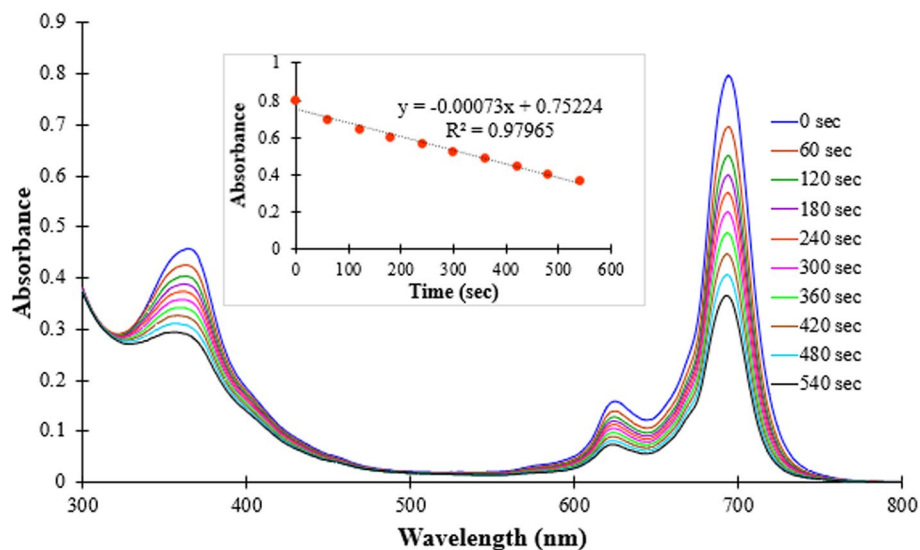
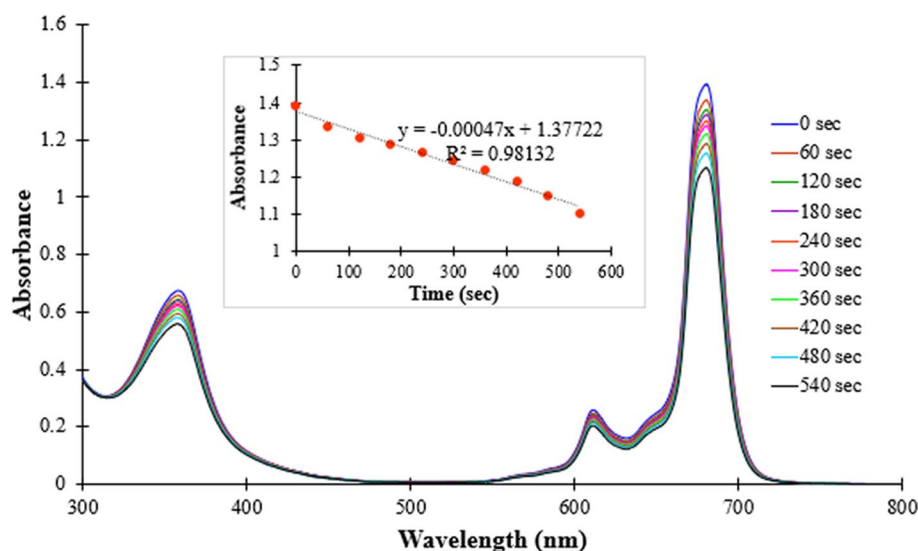


Fig. 8 Electronic absorption spectral changes during the investigation of the photodegradation quantum yield of 2,9,16,23-tetrachloro-3,10,17,24-tetrakis(2-isopropyl-5-methylphenoxy)phthalocyaninato lutetium(III)acetate (**4**) in DMF, $C = 1 \times 10^{-5}$ M



Conclusion

In this study, new metal-free phthalocyanine [**H₂Pc2**] and metallo-phthalocyanines [**In(OAc)Pc 3**, **Lu(OAc)Pc 4**, **ZnPc 5** and **MgPc 6**] containing chlorine and biologically active thymol groups with oxo-bridges were synthesized. Structural characterizations were carried out with the common spectroscopic techniques including FTIR, ¹H- and ¹³C-NMR (for phthalonitrile derivative), UV-Vis, MALDI-TOF spectrometry and elemental analysis as well. The Pcs (**2–6**) showed well solubility without aggregation in commonly known solvents, such as hexane, DCM, CHCl₃, acetone, toluene, DMF, DMSO, and THF, and were also capable of absorbing at maximum intensity at long wavelengths. Photophysical and photochemical experiments of the Pcs have been carried out in DMF because the studied phthalocyanines do not exhibit any aggregates in this solvent. Fluorescence spectra of the studied compounds indicate lower quantum yield in comparison with the **unsubstituted ZnPc** except for **MgPc**. **In(OAc)Pc**, **Lu(OAc)Pc**, and **ZnPc** showed higher singlet oxygen yield compared to standard unsubstituted zinc phthalocyanine. **In(OAc)Pc** showed the highest singlet oxygen quantum yield. Photodegradation studies have shown that the Pcs (**2–6**) have suitable stability against to light irradiation for PDT applications. The singlet oxygen quantum yields, which give indication of the potential of the studied phthalocyanines as photosensitizers in applications where singlet oxygen is required, are suitable for PDT applications of the studied Pcs especially **In(OAc)Pc**.

Supplementary Information The online version contains supplementary material available at <https://doi.org/10.1007/s11243-023-00525-y>.

Acknowledgements We are grateful to the Research Foundation of Marmara University, Commission of Scientific Research (BAPKO)

for their support of this research as part of the project: FEN-C-YLP-120418-0164. In addition, we are very grateful to Assoc. Prof. Dr. Mehmet Pişkin for his skillful and fruitful collaboration.

Author contributions RA performed the synthesis, purification, and characterization of the starting compound and phthalocyanines in the article and write the manuscript. KK performed the photophysical and photochemical characterization of the phthalocyanines in the article. MD and ZO reviewed the manuscript.

Funding Not applicable.

Data and material availability Not applicable.

Declarations

Conflict of interest The authors declare that they have no known competing financial interest or personal relationships that could have appeared to influence the work reported in this paper.

Ethical approval Not applicable.

References

- Crucius G (2013) Synthesen nichtperipher glykokonjugierter Zink (II) phthalocyanine. Universitätsbibliothek Tübingen
- Josefsen LB, Boyle RW (2012) Unique diagnostic and therapeutic roles of porphyrins and phthalocyanines in photodynamic therapy, imaging and theranostics. *Theranostics* 2:916
- Hamblin MR, Hasan T (2004) Photodynamic therapy: a new antimicrobial approach to infectious disease? *Photochem Photobiol Sci* 3:436–450
- Patrice T (2003) Photodynamic therapy. Royal Society of Chemistry, London
- Hirth A, Michelsen U, Wöhrle D (1999) Photodynamische tumortherapie. *Chem unserer Zeit* 33:84–94
- Whitacre CM, Feyes DK, Satoh T, Grossmann J, Mulvihill JW et al (2000) Photodynamic therapy with the phthalocyanine

- photosensitizer Pc 4 of SW480 human colon cancer xenografts in athymic mice. *Clin Cancer Res* 6:2021–2027
7. Allen CM, Sharman WM, Van Lier JE (2001) Current status of phthalocyanines in the photodynamic therapy of cancer. *J Porphyr Phthalocyanines* 5:161–169
 8. Dolmans DE, Fukumura D, Jain RK (2003) Photodynamic therapy for cancer. *Nat Rev Cancer* 3:380–387
 9. Brasseur N (2003) Sensitizers for PDT: phthalocyanines. In: Patrice T (ed) *Photodynamic therapy*, vol 2. The Royal Society of Chemistry, London, pp 105–118
 10. Flom SR (2003) Nonlinear optical properties of phthalocyanines. In: Kadish KM, Smith KM, Guillard R (eds) *The porphyrin handbook. Application of phthalocyanines*. Elsevier Academic Press, California, pp 179–190
 11. Tanaka M (2009) Phthalocyanines – high performance pigments and their applications. In: Faulkner EB, Schwartz RJ (eds) *High performance pigments*. John Wiley and Sons, Weinheim, pp 275–291
 12. Wöhrle D, Schnurpfeil G (2003) Porphyrins and Phthalocyanines in *Macromolecules-110*. In: *The Porphyrin Handbook*. Academic Press, Amsterdam
 13. Mckeown N, Weinreb S (2004) *Science of Synthesis. Houben-Weyl Methods of Molecular Transformations–Hetarenes and Related Ring Systems*. 17: 1237
 14. Seikel E (2012) Axial funktionalisierte Metallophthalocyanine und-porphyrazine als Funktionsmoleküle für optoelektronische Anwendungen. *Philipps-Universität Marburg*
 15. Wöhrle D, Eskes M, Shigehara K, Yamada A (1993) A Simple synthesis of 4, 5-disubstituted 1, 2-dicyanobenzenes and 2, 3, 9, 10, 16, 17, 23, 24-octasubstituted phthalocyanines. *Synthesis* 1993:194–196
 16. Atalay Ş, Çoruh U, Akdemir N, Açar E (2004) C–H \cdots π interactions in 4, 5-bis (2-isopropyl-5-methylphenoxy) phthalonitrile. *Acta Crystallogr Sect E: Struct Rep Online* 60:o303–o305
 17. Nyokong T (2007) Effects of substituents on the photochemical and photophysical properties of main group metal phthalocyanines. *Coord Chem Rev* 251:1707–1722
 18. Becker HG, Böttcher H, Dietz F, Rehorek D, Roewer G et al. (1983) *Einführung in die Photochemie*. Thieme Stuttgart
 19. Klessinger M (1989) *Physikalische organische Chemie*. Verlag Chemie
 20. Grofcsik A, Baranyai P, Bitter I, Csokai V, Kubinyi M et al (2004) Triple state properties of tetrasubstituted zinc phthalocyanine derivatives. *J Mol Struct* 704:11–15
 21. Kumbhar PP, Dewang PM (2001) Eco-friendly pest management using monoterpenoids. I. Antifungal efficacy of thymol derivatives. *J Sci Ind Res* 60:645–648
 22. Li Y, Wen J-m, Du C-j, Hu S-m, Chen J-x et al (2017) Thymol inhibits bladder cancer cell proliferation via inducing cell cycle arrest and apoptosis. *Biochem Biophys Res Commun* 491:530–536
 23. Botelho M, Nogueira N, Bastos G, Fonseca S, Lemos T et al (2007) Antimicrobial activity of the essential oil from *Lippia sidoides*, carvacrol and thymol against oral pathogens. *Braz J Med Biol Res* 40:349–356
 24. Braga PC, Dal Sasso M, Culici M, Bianchi T, Bordoni L, Marabini L (2006) Anti-inflammatory activity of thymol: inhibitory effect on the release of human neutrophil elastase. *Pharmacology* 77:130–136
 25. Aeschbach R, Löliger J, Scott B, Murcia A, Butler J et al (1994) Antioxidant actions of thymol, carvacrol, 6-gingerol, zingerone and hydroxytyrosol. *Food Chem Toxicol* 32:31–36
 26. Ma C, Tian D, Hou X, Chang Y, Cong F et al (2005) Synthesis and characterization of several soluble tetraphenoxy-substituted copper and zinc phthalocyanines. *Synthesis* 2005:741–748
 27. Sobotta L, Lijewski S, Długaszewska J, Nowicka J, Mielcarek J, Goslinski T (2019) Photodynamic inactivation of *Enterococcus faecalis* by conjugates of zinc(II) phthalocyanines with thymol and carvacrol loaded into lipid vesicles. *Inorg Chim Acta* 489:180–190
 28. Görlach B, Dachtler M, Glaser T, Albert K, Hanack M (2001) Synthesis and separation of structural isomers of 2(3),9(10),16(17),23(24)-tetrasubstituted phthalocyanines. *Chem A Eur J* 7:2459–2465
 29. Atajanov R, Huraibat B, Odabaş Z, Özkaya AR (2023) Electrochemical, spectroelectrochemical, and electrocatalytic properties of novel soluble phthalocyanines containing peripheral thymoxy and chloride units. *Inorg Chim Acta* 547:121360
 30. Fernandez JM, Bilgin MD, Grossweiner LI (1997) Singlet oxygen generation by photodynamic agents. *J Photochem Photobiol B* 37:131–140
 31. Kubiak R, Janczak J, Ślędz M, Bukowska E (2007) Comparative study of beryllium, magnesium and zinc phthalocyanine complexes with 4-picoline. *Polyhedron* 26:4179–4186

Publisher's Note Springer Nature remains neutral with regard to jurisdictional claims in published maps and institutional affiliations.

Springer Nature or its licensor (e.g. a society or other partner) holds exclusive rights to this article under a publishing agreement with the author(s) or other rightsholder(s); author self-archiving of the accepted manuscript version of this article is solely governed by the terms of such publishing agreement and applicable law.